

Thermal Conductivity of Al₂O₃ Ceramics: A Discussion on the Application of Kitayama Model to the Thermal Conductivity of Al₂O₃ Ceramics

Shigetaka Wada, Sirithan Jiemsirilers and Supatra Jinawath*

A model estimating the thermal conductivity of silicon nitride ceramics with a grain boundary glassy phase proposed by Kitayama et al. was slightly modified and combined with a Eucken model. The model derived from the combination was used to estimate the thermal conductivity of alumina ceramics in this paper. The coincidence of the thermal conductivity estimated by this model with the measured data was better than that of the Eucken model that assumed no grain boundary morphology.

Key words: thermal conductivity models and alumina ceramics.

การนำความร้อนของอลูมินาเซรามิกส์: การอภิปรายผลของการนำ โมเดลของ Kitayama มาใช้ในการคำนวณค่าการนำความร้อนของ อลูมินาเซรามิกส์

ชigetaka Wada, Sirithan Jiemsirilers และ Supatra Jinawath (2548)

วารสารวิจัยวิทยาศาสตร์ จุฬาลงกรณ์มหาวิทยาลัย 30(2)

โมเดลของ Kitayama สำหรับการคำนวณค่าการนำความร้อนของซิลิคอนไนไตรด์เซรามิกส์ ที่มีเฟสของแก้วตรงบริเวณขอบเกรน ถูกนำมาดัดแปรและประยุกต์ร่วมกับโมเดลของ Eucken ในการหาค่าการนำความร้อนของอลูมินาเซรามิกส์ในงานวิจัยนี้ พบว่าการนำความร้อนที่ได้จากการคำนวณโดยใช้โมเดลประยุกต์ มีค่าใกล้เคียงกับค่าที่ได้จากการทดลองดีกว่าค่าที่ได้จากการคำนวณโดยใช้โมเดลของ Eucken ซึ่งไม่รวมเฟสของแก้วตรงบริเวณขอบเกรน

คำสำคัญ โมเดลการนำความร้อน อลูมินาเซรามิกส์

INTRODUCTION

Al₂O₃ ceramics were sintered without adding flux components and the thermal conductivity (hereafter abbreviated as TC) of the specimens was measured by the Laser Flash method.⁽¹⁻³⁾ The measured TC data were compared with a model of a composite which was composed of a continuous matrix with a dispersed second phase.⁽⁴⁾ In references 1-3, the matrix phase was Al₂O₃ and the dispersed phase was ZrO₂ particles or pores. However, the coincidence of the measured data with the calculated values from the Eucken model was not so good.⁽⁴⁾

Kitayama M., Hirao K., Toriyama M. and Kanzaki S. (hereafter written only the name, Kitayama) proposed a model which was applied to the TC of Si₃N₄ ceramics with glassy grain boundary films and glass pockets.⁽⁵⁾ They reported that the experimental results coincided well with the estimated values of the model.^(5,6)

In our previous paper,⁽⁴⁾ it was assumed that there was no grain boundary film in the Al₂O₃ specimens because no flux was added. However, a small amount (< 0.5 wt%) of impurities (*i.e.* SiO₂, Fe₂O₃ and Na₂O)⁽⁷⁾ in the as-purchased raw powder might form a very thin grain boundary film. Thus, the same thermal conductivity data were compared with the

calculated TC values based on Kitayama model in this paper.

MODELING

General formula

Simple thermal conductivity models of a composite depict a series of slabs and parallel slabs. Series slab models mean the structures of the two phases are in series and the direction of heat conduction is perpendicular to them. In parallel models, the direction of heat conduction is parallel to the plane of the slabs.⁽⁸⁾ The equations of thermal conductivity for these models are quoted in the Appendix.

Figure 1 shows an idealized three dimensional model composed of grains with a thin layer of a grain boundary phase as the continuous phase and some amounts of glass pockets in between grains as the dispersed phase. This is the same model proposed by Kitayama *et.al.*⁽⁵⁾ In the Kitayama model, a rectangular grain was assumed, but in this paper, a cubic grain is assumed. The continuous phase of Figure 1 can also be treated as a composite with grain boundary and its thermal conductivity, $\kappa c'$, can be expressed by equation (1), the details are given in the Appendix.

$$\kappa c' = \frac{\kappa_G \{l\kappa_A + \delta(\kappa_A + 2\kappa_G)\}}{l\kappa_G + \delta(\kappa_A + 2\kappa_G)} \quad \dots (1)$$

According to Eucken,⁽⁵⁾ Figure 1 is simply considered as the composite of only 2 phases, a continuous phase and the dispersed phase (no

grain boundary involved). The TC of such composite, κ_m , is as shown in equation (2).

$$\kappa_m = \kappa_c \frac{1 + 2v_d(1 - \kappa_c / \kappa_d) / (2\kappa_c / \kappa_d + 1)}{1 - v_d(1 - \kappa_c / \kappa_d) / (2\kappa_c / \kappa_d + 1)} \quad \dots (2)$$

κ_c and κ_d are the TCs of the continuous and discontinuous phases, respectively. And v_d is the

volume fraction of the discontinuous phase.

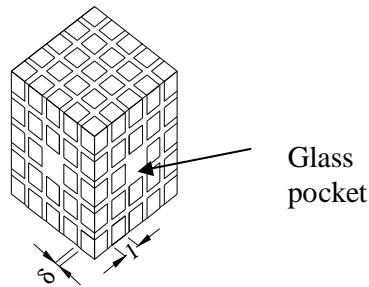


Figure 1(a). Three dimensional microstructure model composed of cubic grains and grain boundary thin layers.

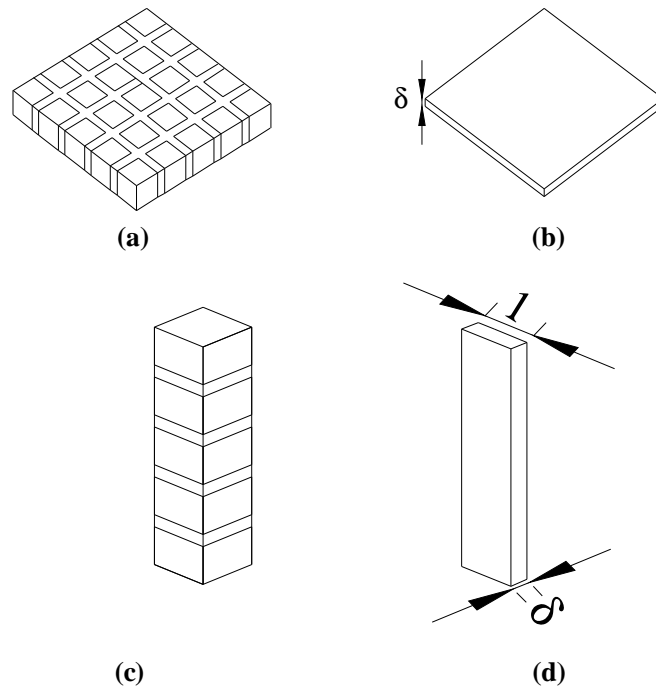


Figure 1(b). Layers taken apart from the three dimensional microstructure model to explain parallel and series calculation, (a) parallel first layer, (b) thin layer series to (a), (c) first series layer and (d) thin layer parallel to (c).

By applying both the Kitayama and Eucken models to the structure of Figure 1, with the assumption that it is the structure of a two phase composite, $\kappa_c = \kappa c'$, and κ_d is the thermal conductivity of the dispersed glass pockets. Thus we arrive at a model including

the grain boundary phase and glass pocket. Practically, it is difficult to estimate the right volume of the glass pocket because some amount of glass phase is consumed as the thin film between grains. Therefore the following procedure is proposed.

When the glass layer is very thin, its thickness, δ , is very small compared with the width of Al₂O₃ grain, l . When the volume of glass is larger than the threshold, glass pockets generate. On the other hand, when δ is not so small and the volume of glass phase is less than that of the threshold, the glass phase does not fill all the grain boundaries. This results in no glass pocket. The total volume of grain boundary phase, v_t , is calculated by the following equation.

$$v_t = 1 - \frac{l^3}{(l + \delta)^3} \quad \dots (3)$$

Assuming l as 1, 10 and 100 μm and δ as 1, 10 and 100 nm , the threshold volume of glass phase (v_t) is calculated and graphically presented in Figure 2. The calculated lines display the limit of the threshold, hence glass pocket will generate when the content of glass phase is above the line.

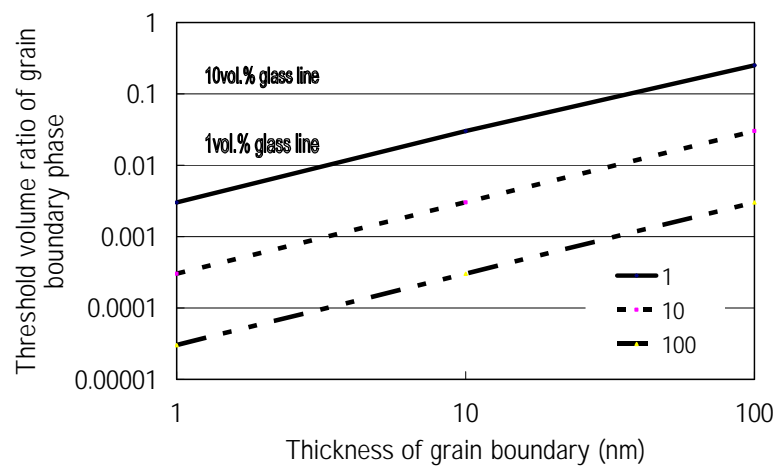


Figure 2. The threshold volume of glassy phase as function of grain size (micro meter) and thickness of grain boundary phase (nano meter).

Calculation premise for Al₂O₃ ceramics

Grain boundary is not only a glass phase, but also a distorted lattice and a high concentration solid solution phase. In this paper, the word “grain boundary” is used as a representative expression for this complexity. Calculation was performed for 1-10 μm of Al₂O₃ grains and in the range of 0-20 nm grain boundary thicknesses. In the following calculation, 40 W/mK and 1 W/mK were used as the TCs at room temperature of Al₂O₃ and grain boundary phases, respectively.

The relationship between TC of Al₂O₃ ceramics as a function of grain boundary thickness plotted according to equation 2 using $v_d = v_t$, is shown in Figure 3. When the

thickness of grain boundary increases from 1 nm to 20 nm, TC of the Al₂O₃ ceramics decreases. The effect is serious when the grain size is as small as 1-2 μm . The relationship between TC of Al₂O₃ ceramics as a function of the grain size of Al₂O₃ was also plotted according to equation 2, shown in Figure 4. In these figures, the amount of glass phase is the amount which fills the grain boundary as a thin film. The effect of grain size on the TC of Al₂O₃ ceramics is clearly illustrated in Figure 4. When grain size is smaller than 5 μm and the thickness of the grain boundary is over 10 nm, TC of Al₂O₃ ceramics decreases drastically.

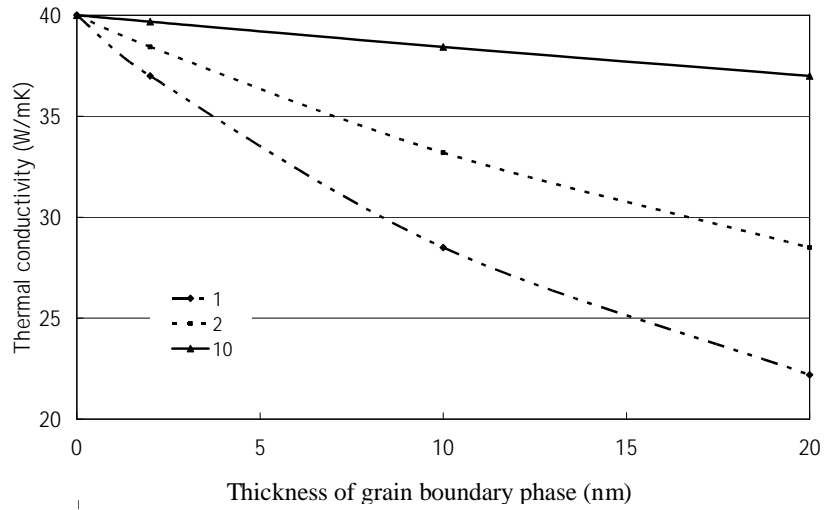


Figure 3. Thermal conductivity of composite as function of grain size and the thickness of grain boundary phase.

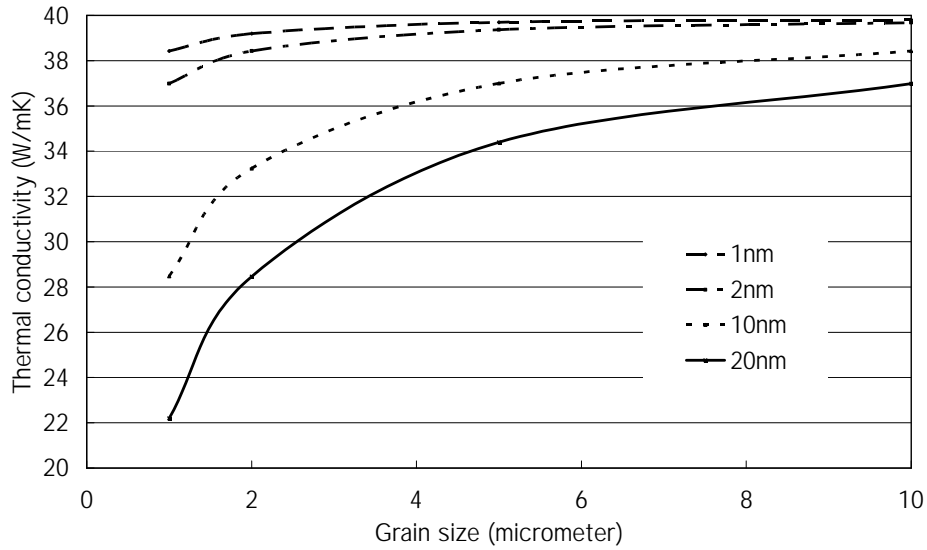
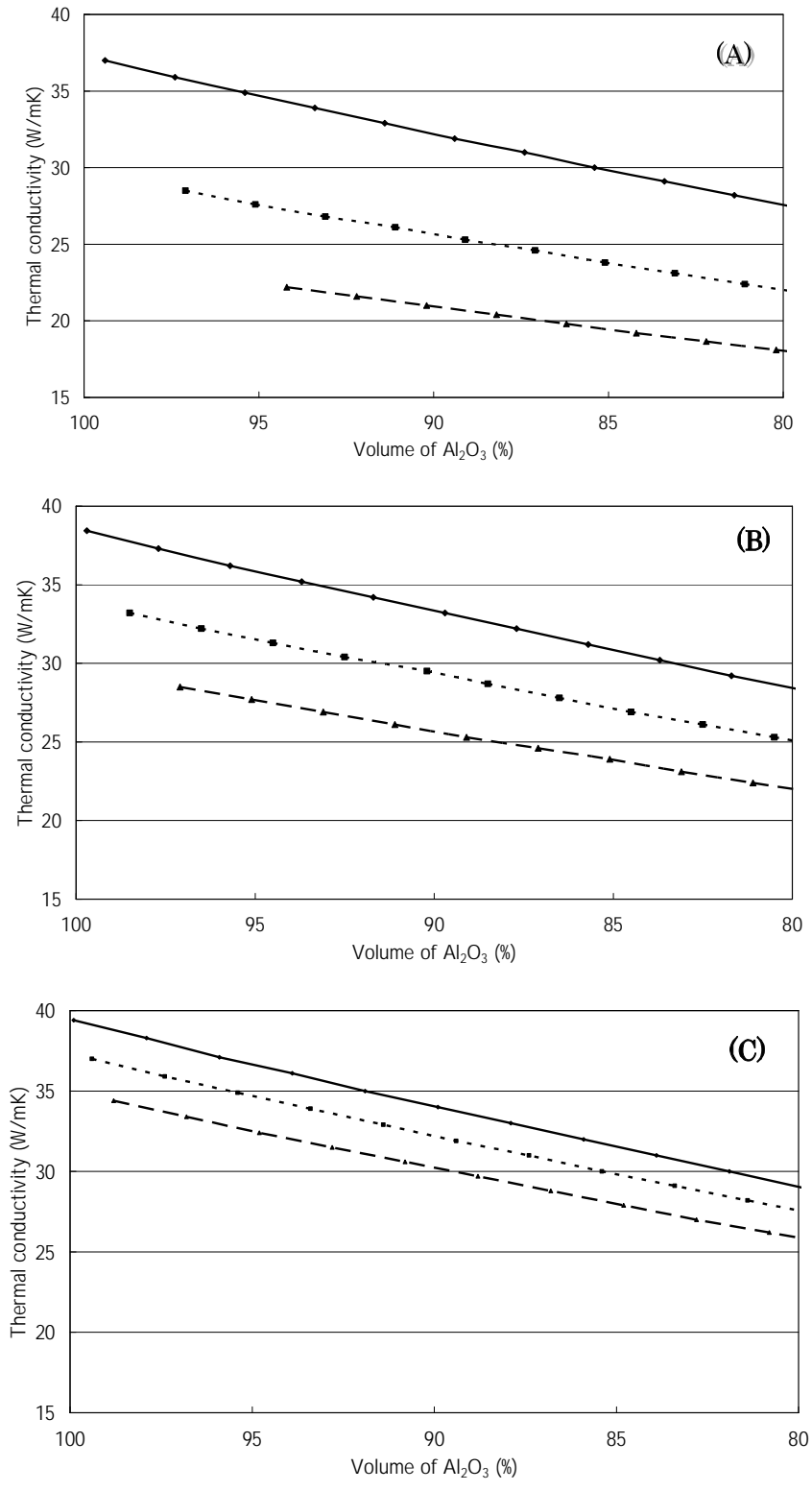


Figure 4. TC of Al₂O₃ as function of grain boundary thickness and grain size.

The properties of ceramics are usually considered a function of the purity of the main material: for example, Al₂O₃ content in the case of Al₂O₃ ceramics. Figure 5 shows the relationship between the TC and the volume percent of Al₂O₃ in the ceramics (plotted according to equation 2, replacing κ_c with κ_c' and treating glass pockets as the dispersed phase). As shown in (A) and (B), TC decreases and threshold grain boundary volume increases with increasing thickness of grain boundary, especially when the grain size is as small as 1-2

μm . Neither TC nor threshold grain boundary volume change much when grain size is larger than 5 μm as shown in (C) and (D). The descending slope of the lines when the volume of Al₂O₃ is decreased shows the effect of the glass pocket content on TC. The angles of slope are not much different from one another. One weak point of the model is that it can not predict the TC in the region where the volume of the grain boundary is less than the threshold. Probably in this case, the TC should have a value between 40 W/mK and that of the threshold point.



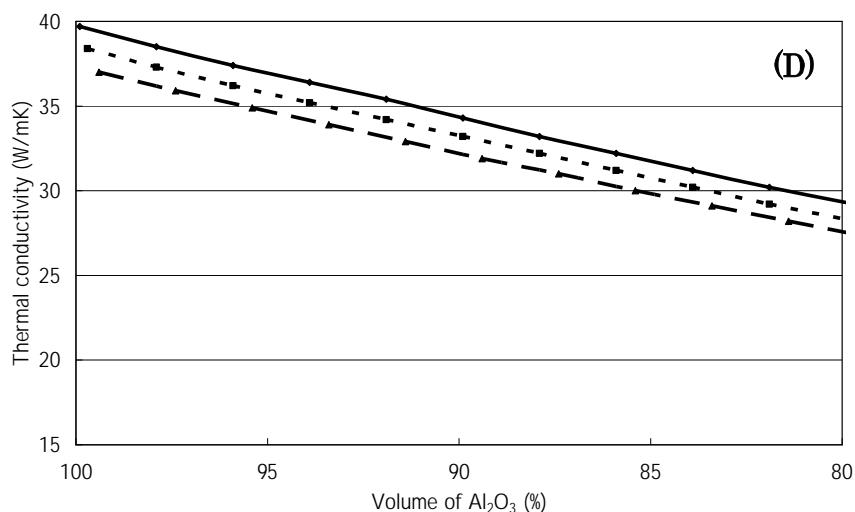


Figure 5. The relationship between the thermal conductivity and volume percentage of Al_2O_3 in the alumina ceramics for the average Al_2O_3 grain size (A) $1\ \mu\text{m}$, (B) $2\ \mu\text{m}$, (C) $5\ \mu\text{m}$ and (D) $10\ \mu\text{m}$. The thickness of grain boundary is $2\ \text{nm}$ (solid line), $10\ \text{nm}$ (dash line) and $20\ \text{nm}$ (long dash line).

DISCUSSION

It was reported that alumina ceramics would sinter by liquid phase sintering when the purity was less than 99.7 wt%.⁽⁹⁾ Generally the impurities in Al_2O_3 powder were SiO_2 and Na_2O (Reference 4, Table 1), hence the grain boundary phase is a glass composed of SiO_2 and Na_2O and the volume of glass phase is estimated to be about 0.6 volume%, because the density of a glass composed of SiO_2 and Na_2O is about $2\ \text{g/cm}^3$ and that of Al_2O_3 is $\sim 4\ \text{g/cm}^3$. However, the report did not define the grain boundary phase exactly.

High purity alumina ceramics were consolidated and the TCs of the specimens were measured. The details of the experimental data were reported in References 1-3 (available at the library of the Faculty of Science, Chulalongkorn University). The coincidence of the experimental values with calculated values from the Eucken model was not so good⁽⁴⁾ because the model was premised on the assumption that no grain boundary is involved. The purities of Al_2O_3 in the two kinds of alumina powder, AKP-30 ($0.3\ \mu$) and AES-11 ($0.5\ \mu$), were 99.99 and 99.80 wt%, respectively. Considering the purity, there would be almost no grain boundary if reference (8) is correct.

It has also been reported that very high purity alumina ceramics, for example 99.995 wt% Al_2O_3 with 300 ppm impurity such as Yttrium, had a grain boundary phase which was

different from the bulk.⁽¹⁰⁾ Other cation impurities such as Mg, Ti also segregated into grain boundary.⁽¹¹⁻¹⁴⁾ The grain boundary thickness was suggested to be $\sim 0.5\ \text{nm}$ ⁽¹²⁾ or $2\ \text{nm}$.⁽¹³⁾ G. C. Wei⁽¹⁴⁾ thought that the relatively large grain-boundary width, $\sim 50\ \text{nm}$, seemed to be reasonable as a chemical-width (chemically different boundary thickness) rather than a structural-width based on reference 15.

As mentioned above, there are several kinds of grain boundary such as glassy phase, other cation segregated thin layer, and boundary layer which are not structurally but chemically different in composition. Sometimes cation segregated in grain boundary also dissolved in the lattice.^(11,13) Considering all the papers mentioned above, it seems that various types of grain boundary tend to give different TC values. However, these papers had not provided any information on TC.

Figure 6 shows a relationship between the thermal conductivity and the volume percentage of Al_2O_3 in alumina ceramics. The plots are drawn from the experimental results and the values premised on the models in the previous section. The plotted lines are calculated for the case in which the grain size of Al_2O_3 is $2\ \mu\text{m}$ and grain boundary thicknesses are 2, 10 and 20 nm. The top line shows the calculated line assuming the Eucken model. As seen in the Figure, based on Kitayama model, the TC values

(●) of specimens synthesized from AKP-30 and sintered at high temperatures (1600 and 1650°C) are close to the calculated line for 2 nm grain boundary. On the other hand, the TC values (△) of specimens synthesized from AES-11 and sintered at the same temperatures are close to

the calculated line for 10 nm grain boundary. The TC values (□) of specimens synthesized from AKP-30 and sintered at lower temperatures (1450 and 1550°C) are also close to the calculated line for 10 nm grain boundary.

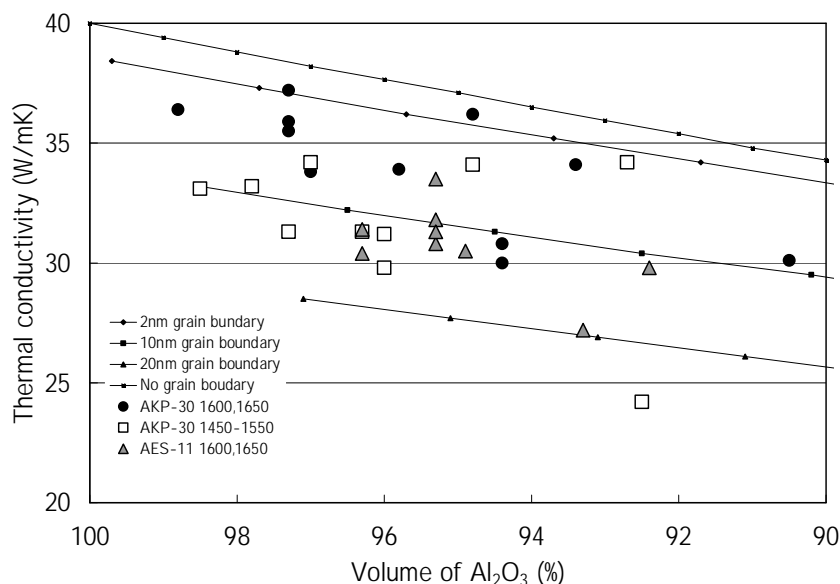


Figure 6. The relationship between the thermal conductivity and the volume percentage of Al₂O₃ in alumina ceramics comparing the experimental results and calculated values from the model when the grain size is 2 μm.

Though the experimental data are close to some of the calculated lines, the morphology of each specimen has not been analyzed in detail since such thickness of grain boundary phase requires a high resolution transmission electron microscope (TEM). Therefore, the coincidence is taken as accidental, and it can not be concluded that the specimens have a grain boundary thickness of 2 nm or 10 nm. Moreover, so far there have been no references of the TC of grain boundary available, so our calculation assumed that the TC of the grain boundary is 1 W/mK. However, there is no proof that this value is reasonable. On the other hand, by changing the grain size of Al₂O₃ and the grain boundary thickness, the model with grain boundary and glass pocket can cover a wide range of TC values. In this sense, the model must be better than that of Eucken.

The TC of alumina ceramics relating to the chemical composition and morphology will be investigated more in detail by the authors in

the near future and will be discussed based on the model.

CONCLUSIONS

A model estimating the thermal conductivity of alumina ceramics based on Kitayama's was proposed. The coincidence of the thermal conductivity estimated by this model with the measured thermal conductivity data was better than the Eucken model that assumed no grain boundary morphology. Though the experimental data are close to some of the calculated lines, the morphology of each specimen has not been analyzed in detail. Therefore, the coincidences are thought to be accidental. However by changing the grain size of Al₂O₃ and grain boundary thickness, the model with grain boundary and glass pocket covers a wide range of TC. In this sense, the model should be more appropriate than the Eucken model.

Appendix: Formulation of the equation to calculate the thermal conductivity (hereafter abbreviated as TC) of a composite having an idealized three dimensional model.

The TC of parallel slab models is calculated by equation (1a).

$$\kappa_c = v_1 \kappa_1 + v_2 \kappa_2 \quad \dots (1a)$$

That of series slab models is calculated by equation (2a).

$$\frac{1}{\kappa_c} = \frac{v_1}{\kappa_1} + \frac{v_2}{\kappa_2} \quad \dots (2a)$$

κ_c is the thermal conductivity of a composite, κ_1, κ_2 are the thermal conductivities and v_1, v_2 are the volume fractions of phases 1 and 2 of the composite, respectively.⁵ These two formulas are applied to calculate the TC of a composite with grain boundary film (but without glass pocket).

The TC of the composite shown in Figure 1 when glass pocket is excluded can be formulated by either one of the two processes. The first process is shown in the Appendix, Figures 1b (a) and (b), and the second is in Figures 1b (c) and (d).

In the first process, at first TC of the parallel composite layer shown in (a), κ_p , is calculated following equation (1a) and shown as equation (3a).

$$\kappa_p = \left(\frac{l}{l+\delta} \right)^2 \kappa_A + \left\{ \frac{(l+\delta)^2 - l^2}{(l+\delta)^2} \right\} \kappa_G \quad \dots (3a)$$

Here, l and δ are the width of the Al_2O_3 grain and the thickness of grain boundary, respectively. κ_A and κ_G are the TCs of Al_2O_3 and grain boundary phase, respectively. Total volume of the composite = $(l+\delta)^2 l$, volume of Al_2O_3 grains = l^3 , and volume of grain boundary = $(l+\delta)^2 l - l^3$. Next, TC of the layer and boundary film shown in (b), κ_{ps} , is calculated following equation (2a) and shown as equation (4a).

$$\frac{1}{\kappa_{ps}} = \left(\frac{l}{l+\delta} \right) \frac{1}{\kappa_p} + \left(\frac{\delta}{l+\delta} \right) \frac{1}{\kappa_G} \quad \dots (4a)$$

Where total volume of the composite = $(l+\delta)^3$, volume of Al_2O_3 grains = $(l+\delta)^2 l$, and volume of grain boundary = $(l+\delta)^2 \delta$.

Substitute κ_p in (4a), and omit the terms containing δ^2 and δ^3 , κ_{ps} is formulated as in equation (5a). The equation shows the TC of the composite having the structure shown in Figure 1, but with no glass pockets.

$$\kappa_{ps} = \frac{\kappa_G \{ l \kappa_A + \delta (\kappa_A + 2\kappa_G) \}}{l \kappa_G + \delta (\kappa_A + 2\kappa_G)} \quad \dots (5a)$$

The second process is shown in Appendix, Figure 1b (c) and (d). At first, by a similar process,

TC of the series composite layer shown in (c), κ_s , is formulated as in equation (6a).

$$\frac{1}{\kappa_s} = \left(\frac{l}{l+\delta} \right) \frac{1}{\kappa_A} + \left(\frac{\delta}{l+\delta} \right) \frac{1}{\kappa_G} \quad \dots (6a)$$

Next, parallel TC of the series composite and grain boundary film shown in (d), κ_{sp} , is formulated as in equation (7a). The structure of this composite is the same as that of (a), but the direction of heat conduction is different.

$$\kappa_{sp} = \left(\frac{l}{l+\delta} \right) \kappa_s + \left(\frac{\delta}{l+\delta} \right) \kappa_G \quad \dots (7a)$$

Then, the composite layer having the TC of κ_{sp} is layered again with grain boundary film. The TC of final composite (κ_{spp}) is formulated in equation (8a).

$$\kappa_{spp} = \left(\frac{l}{l+\delta} \right) \kappa_{sp} + \left(\frac{\delta}{l+\delta} \right) \kappa_G \quad \dots (8a)$$

Substitute κ_s in equation (7a) and κ_{sp} in equation (8a), then κ_{spp} is formulated. The details of the substitute and calculation were omitted here. Finally, the equation of κ_{spp} is the same as that of κ_{ps} shown in equation (5a).

ACKNOWLEDGMENTS

The authors would like to acknowledge the financial support of AISIN SEIKI Co. Ltd.,

Japan and the research facilities provided by Chulalongkorn University.

REFERENCES

- Piempermpoon, B. (2002) "Improvement of thermal conductivity of alumina for peltier element" MS thesis, Department of Materials Science, Faculty of Science, Chulalongkorn University, ISBN 974-17-0850-5.
- Na Nakorn, P. (2003) "Development of alumina substrate for peltier element" MS thesis, Department of Materials Science, Faculty of Science, Chulalongkorn University, ISBN 974-17-4458-7.
- Na Nakorn, P., Jinawath, S., and Wada, S. (2005) "Mechanical strength and thermal conductivity of high purity Al₂O₃ ceramics using AKP-30 Powder" *J. Sci. Res. Chula Univ.* **30(1)**, 77-85.
- Wada, S., Piempermpoon, B., Na Nakorn, P., Wasanapiarnpong, T. and Jinawath, S. (2005) "Thermal conductivity of Al₂O₃ ceramics: The inconsistency between measured value and calculated value based on analytical models of a composite" *J. Sci. Res. Chula Univ.* **30(1)**, 109-120.
- Kitayama, M., Hirao, K., Toriyama, M. and Kanzaki, S. (1999) "Thermal conductivity of β -Si₃N₄: α , Effect of various microstructural factors" *J. Am. Ceram. Soc.* **82(11)**, 3106-3112.
- Kitayama, M., Hirao, K., Tsuge, A., Watari, K., Toriyama M., and Kanzaki, S. (2000) "Thermal conductivity of β -Si₃N₄: α , effect of lattice oxygen" *J. Am. Ceram. Soc.* **83(8)**, 1985-1992.
- Gitzen, W. H. (1976) "Alumina as a ceramic material" *American Ceramic Society*, 20-26.
- Kingery, W. D., Bowen, H. K., and Uhlmann, D. W. (1976) "Introduction to ceramics" 2nd edition, 634-636.
- Lee, W. E., and Rainforth, W. M. (1994) "Ceramic microstructure: property control by processing" *Chapman & Hall*, 269.
- Voytovych, R., MacLaren, I., Gulgun, M. A., Cannon, R. M. and Ruhle, M. (2002) "The effect of yttrium on densification and grain growth in α -alumina" *Acta Materialia* **50**, 3453-3463.

11. Roy, S. K. and Coble, R. L. (1968) "Solubilities of magnesia, titania, and Magnesium titanate in aluminum oxide" *J. Am. Ceram. Soc.*, **51(1)**, 1-6.
12. Bae, I. J. and Baik, S. (1997) "Abnormal grain growth of alumina" *J. Am. Ceram. Soc.* **80(5)**, 1149-1156.
13. Gavrilov, K. L., Bennison, S. J., Mikeska, K. R. and Levi-Setti, R. (1999) "Grain boundary chemistry of alumina by high-resolution imaging SIMS" *Acta mater.* **47(15)**, 4031-4039.
14. Wei, G. C., (2004) "Grain growth and sintering of translucent polycrystalline alumina" *J. Ceram. Soc. Japan* **112(5)**, S179-S182.
15. Wang, C. M., Cargill III, G. S., Chan, H. M. and Harmer, M. P. (2000) "Structural features of Y-saturated and supersaturated grain boundaries in alumina" *Acta mater.* **48**, 2579-2591.

Received: June 16, 2005

Accepted: September 19, 2005